Electrocatalysis Study of Biological Molecules and Oxides Using Nanocomposite of Polyaniline and Silicomolybdate Hybrid Film

Kuo-Chiang Lin, Xiao-Cheng Jian, Shen-Ming Chen[*]

Electroanalysis and Bioelectrochemistry Lab,Department of Chemical Engineering and Biotechnology, National Taipei University of Technology, No.1, Section 3, Chung-Hsiao East Road, Taipei 106, Taiwan (ROC).
[*]E-mail: smchen78@ms15.hinet.net

A nanocomposite of polyaniline and silicomolybdate has been successfully co-deposited on electrode surface by aniline electropolymerization and the electrostatic interaction between the positive charge polyaniline and the negative charge silicomolybdate. The hybrid composite is found stable in various scan rate and different pH condition. The UV-Visible spectrum also shows no other interaction occurred in both the prepared solution and the hybrid film. Images study might provide that silicomolybdate covers over the polyaniline polymerized layer. Under 20 scan cycles, the average surface concentration (Γ) was estimated to be about 1.37×10^{-10} mol cm^{-2}. Using the equation $E_p = K - 2.303(RT/nF)\log v$ and the two electrons transferred for polyaniline a charge transfer coefficient 0.60 was obtained. An apparent surface electron transfer rate constant (K_s) 1.878 s^{-1} was estimated for reversible redox peaks. This modified electrode maintains both electrocatalytic oxidation and reduction properties to AA, DA, EP, NEP, BrO_3^-, IO_3^-, NO_2^-, and $S_2O_8^{2-}$. Particularly, the electrocalysis is much better in strong acidic aqueous solution (pH 0.55). Applied potential of $E_R = 1.1$ V (pH 1.5), the collection efficiency, $N = I_R/I_D$, was about 0.08.

Keywords: Electrocatalysis, biological molecules, oxides, polyaniline, silicomolybdate

1. INTRODUCTION

Among the conducting polymers, polyaniline (PANI) has attracted attention of most of the researchers, due to the combination of unique properties like simple preparation and doping procedure, good environmental stability, relatively high conductivity and low cost and also due to their wide spectrum of applications [1, 2]. Due to its chemical, electrical, and optical properties, PANI has been widely studied and used in rechargeable batteries [3, 4] and electrocatalysis [5-11]. However, the strict demands for medium acidity (pH < 4) limit the potential applications of PANI, especially in

bioelectrochemistry, which normally requires a neutral pH environment. To develop the extensive application of PANI, many efforts have been focused on the adaptation of PANI to a higher solution pH. Following the first introduction of sulfonic acid group into PANI backbone to get the self-doped PANI [12], which can maintain its electroactivity in neutral pH, many researchers tried to prepare sulfonated PANI including copolymerization of aniline with sulfonated aniline or organic acid or homopolymerization of ring sulfonated aniline by substituting with electron donating groups or by putting a spacer between the sulfonated group and the ring [13-16]. Recently, Zhang et al. have studied the synthesis of self-doped PANI via electrochemical copolymerization of aniline and o-aminobenzenesulfonic acid [9] or oaminophenol [8] and their applications for the electrocatalytic oxidation of ascorbic acid (AA).

Silicomolybdate (SiMO) polyoxometalate, $SiMo_{12}O_{40}^{4-}$, form nanometer-sized polyoxometalate clusters that are of interest in bioanalysis, material science, catalysis, magnetism, surface chemistry and medicine. The polyoxometalate anion is a mixed-valence species and polyoxometalate modified electrodes and their electrocatalytic properties are very important and are the subject of intensive research. Some polyoxometalate modified electrodes have been reported in the literature concerning nanostructured organic and inorganic hybrid films [17–25].

Catecholamine plays an important role as neurotransmitters in the central nervous system [26]. Accurate and selective measurements of catecholamines such as dopamine (DA), epinephrine (EP), norepinephrine (NEP), and serotonin (SE) in biological samples are important for both clinical diagnosis and pathological study of certain diseases. In clinical chemistry, measurements of urinary free catecholamines (UFCA) are widely regarded as a sensitive and specific screening test to detect brain tumors as pheochromocytoma and neuroblastoma [27]. It also provides additional records that help detect heart and circulatory diseases (e.g. congestive heart failure, hypertension) as well as diabetes mellitus [28]. Due to their transmitter function in the brain, the catecholamine concentrations in body fluids can serve as a biochemical indicator of several neurological disorders including learning and memory formation, and they are useful in the investigation of the pathological processes of Parkinson's disease [29] and also they have been increasingly utilized to assess the effects of exposure to occupational stress [30]. The analytical methods employed for the determination of EP are based on chromatographic techniques using different detection systems [31, 32]. These methods do not easily allow continuous "in situ" analysis and often require several previous sample preparation steps, which include an extraction and clean-up procedure in order to obtain a final extract fully compatible with chromatographic determination. These techniques usually generate waste-containing organic solvents, which make the procedure more complicated and expensive. Electrochemical methods have a number of advantages as: low cost; high sensitivity; easy operation; the potential for miniaturization and automation; allow the construction of simple portable devices for fast screening purposes; and in-field/on-site monitoring. Nevertheless, a major problem in electrochemical determination of catecholamines is the interference of AA and UA. Moreover, AA and UA are oxidized at almost the same potential as catecholamines. As a result, an unwanted voltammetric response (overlapping) for the oxidation of UA and AA is usually obtained. Also, large overpotential values for such oxidations and fouling of the electrode surface by the electrochemical products of catecholamines oxidation pose difficulties in voltammetric determination [33].

In this work, we report a simple method to immobilize PANI and SiMO on electrode surface for electrocatalysis study including the electrocatalytic oxidation of AA, DA, EP, NEP and the electrocatalytic reduction of BrO_3^-, IO_3^-, NO_2^- and $S_2O_8^{2-}$. The hybrid films were electro-codeposited by the aniline electropolymerization and the electrostatic interaction between PANI and SiMO. The electrochemical behaviors, surface morphology, and electrocatalytic properties were investigated by cyclic voltammetry, scanning electron microscopy, atomic force microscopy, UV-Vis spectroscopy, and rotating ring-disk electrode voltammetry, respectively.

2. EXPERIMENTAL

2.1. Reagents

Aniline monomer, silicomolybdate (SiMO), ascorbic acid (AA), dopamine (DA), epinephrine (EP), norepinephrine (NEP), nicotinamide adenine dinucleotide (NADH), potassium chlorate ($KClO_3$), potassium bromate ($KBrO_3$), potassium iodate (KIO_3), sodium nitrite ($NaNO_2$), and potassium persulfate ($K_2S_2O_8$) were purchased from Sigma-Aldrich (USA).

All other chemicals (Merck) used were of analytical grade (99%). Double distilled deionized water (DDDW) was used to prepare all the solutions. Both pH 0.55 (0.1 M H_2SO_4) and pH 1.5 (0.1 M H_2SO_4) was prepared using sulfuric acid to dilute with DDDW. A pH 4 buffer solution was prepared using potassium hydrogen phthalate (0.1 M KHP). A phosphate buffer solution (PBS) of pH 7 was prepared using Na_2HPO_4 (0.05 M) and NaH_2PO_4 (0.05 M). Other higher pH buffer solutions were appropriately adjusted with di-sodium tetraborate, sodium carbonate, and sodium hydroxide, respectively.

2.2. Apparatus

All electrochemical experiments were performed using CHI 1205a potentiostats (CH Instruments, USA). The BAS glassy carbon electrode (GCE) with a diameter of 0.3 cm and exposed geometric surface area of 0.07 cm^2 (purchased from Bioanalytical Systems, Inc., USA) was used. A conventional three-electrode system was used which consists of an Ag/AgCl (3M KCl) as a reference electrode, a GCE as a working electrode, and a platinum wire as a counter electrode. For the rest of the electrochemical studies, an Ag/AgCl (3M KCl) was used as a reference. Prior to the experiments, the glassy carbon electrode was ultrasonicated in DDDW for 1 min after finishing the polish by Buehler felt pads and alumina power (0.05 μm).

The morphological characterization of composite films was examined by means of SEM (S-3000H, Hitachi) and AFM (Being Nano-Instruments CSPM-4000, China). The AFM images were recorded with multimode scanning probe microscope. Indium tin oxide (ITO) glass was the substrate coated with different films for AFM analysis. The buffer solution was entirely altered by deaerating with nitrogen gas atmosphere. The electrochemical cells were kept properly sealed to avoid the oxygen interference from the atmosphere.

2.3. Electrochemical preparation of PANI/SiMO hybrid film

The electrochemical formation of the PANI/SiMO hybrid film was performed by repetitive cycling of the potential of the working electrode in a definite potential between -0.2 V and 0.85 V in a pH 1.5 aqueous solution containing the aniline monomer and silicomolybdate molecules.
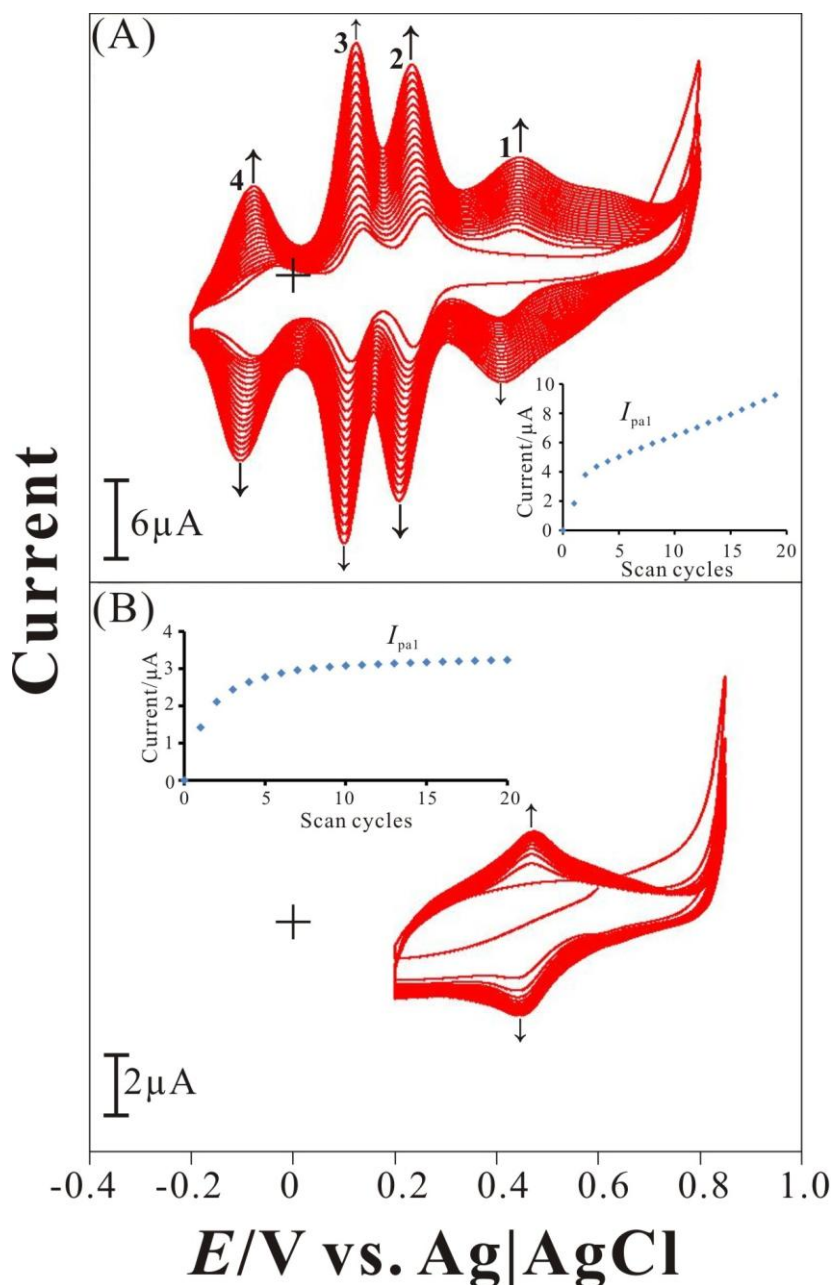

Figure 1. (A) Cyclic voltammograms of poly(aniline) and SiMO co-deposited on glassy carbon electrode in 0.1 M sulfuric solution (pH 1.5) containing 4×10^{-3} M aniline and 1×10^{-4} M SiMO with 20 scan cycles and scan rate of 0.1 V s^{-1} (four redox couples were marked of 1-4 in the order from positive to negative potential). (B) Cyclic voltammograms of PANI electrodeposited on glassy carbon electrode in 0.1 M sulfuric solution (pH 1.5) containing 4×10^{-3} M aniline with 20 scan cycles and scan rate of 0.1 V s^{-1}. Insets were the plot of anodic peak current (I_{pa1}) versus scan cycles.

3. RESULTS AND DISCUSSION

3.1. Preparation of PANI/SiMO hybrid film

PANI and SiMO hybrid film can be prepared on electrode surface using GCE in acidic aqueous solution. The hybrid film was abbreviated as PANI/SiMO for convenience. Fig. 1A displays the voltammograms of PANI/SiMO film growth using GCE with 20 scan cycles and scan range of -0.2$-$0.8 V in 0.1 M H_2SO_4 solution (pH 1.5) containing 4×10^{-3} M aniline monomer and 1×10^{-4} M SiMO. Four redox couples were found with formal potential ($E^{0'}$) of $E_1^{0'} = 0.428$ V, $E_2^{0'} = 0.235$ V, $E_3^{0'} = 0.127$ V, and $E_4^{0'} = -0.080$ V. The redox couple 1 is known for polyaniline redox process as shown in Scheme 1) as compared with the voltammograms (Fig. 1B) of PANI film growth using GCE in 0.1 M H_2SO_4 solution (pH 1.5) containing 2×10^{-3} M aniline.
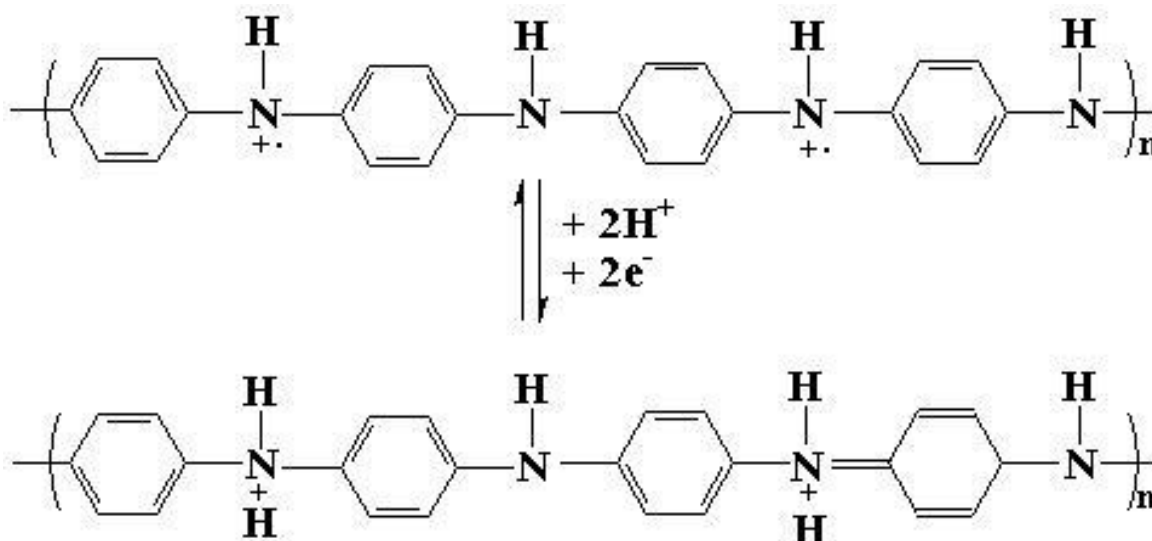
Scheme 1. The electrochemical process of PANI polymer peak.

Other three redox couples are known for SiMO redox process, viz. ($[H_4SiMo_{12}O_{40}]/[H_6SiMo_{12}O_{40}]$, $[H_6SiMo_{12}O_{40}]/[H_8SiMo_{12}O_{40}]$, $[H_8SiMo_{12}O_{40}]/[H_{10}SiMo_{12}O_{40}]$ of the $SiMo_{12}O_{40}^{4-}$ redox process [34], in the cyclic voltammograms. In the first scan cycle in Fig. 1A, it is noticed that the PANI redox peaks do not appear due to PANI is not formed yet. PANI redox peaks are getting obviously after first scan cycle because the electropolymerization occurs with enough positive potential to oxidize aniline to form PANI when scan to 0.8 V. At the same time, the negative charge of SiMO is induced and co-deposited with the positive charge of PANI which has been immobilized on electrode surface. Therefore, the current devolvement of four redox peaks is found in the cyclic voltammograms (Fig. 1A). The current development is linearly dependent on scan cycles (inset of Fig. 1A). It is a simple and convenient method to prepare PANI/SiMO hybrid film. One can conclude that the hybrid film formation is based on aniline electropolymerization inducing SiMO co-deposition.

3.2. Electrochemical characteristics of PANI/SiMO

In the present paper, PANI and SiMO hybrid film (PANI/SiMO) was firstly modified onto the electrode surface by electro-codeposition. The electrochemical properties of PANI/SiMO modified GCE were studied with various scan rates and pH solutions by cyclic voltammetry. Fig. 2 shows the cyclic voltammograms of the resulting electrode obtained with various scan rates in 0.1 M H$_2$SO$_4$ solution (pH 1.5). The electrochemical response of PANI/SiMO/GCE exhibits four stable redox couples, in which can be attributed to the electron transformations between PANI and SiMO in the hybrid film.
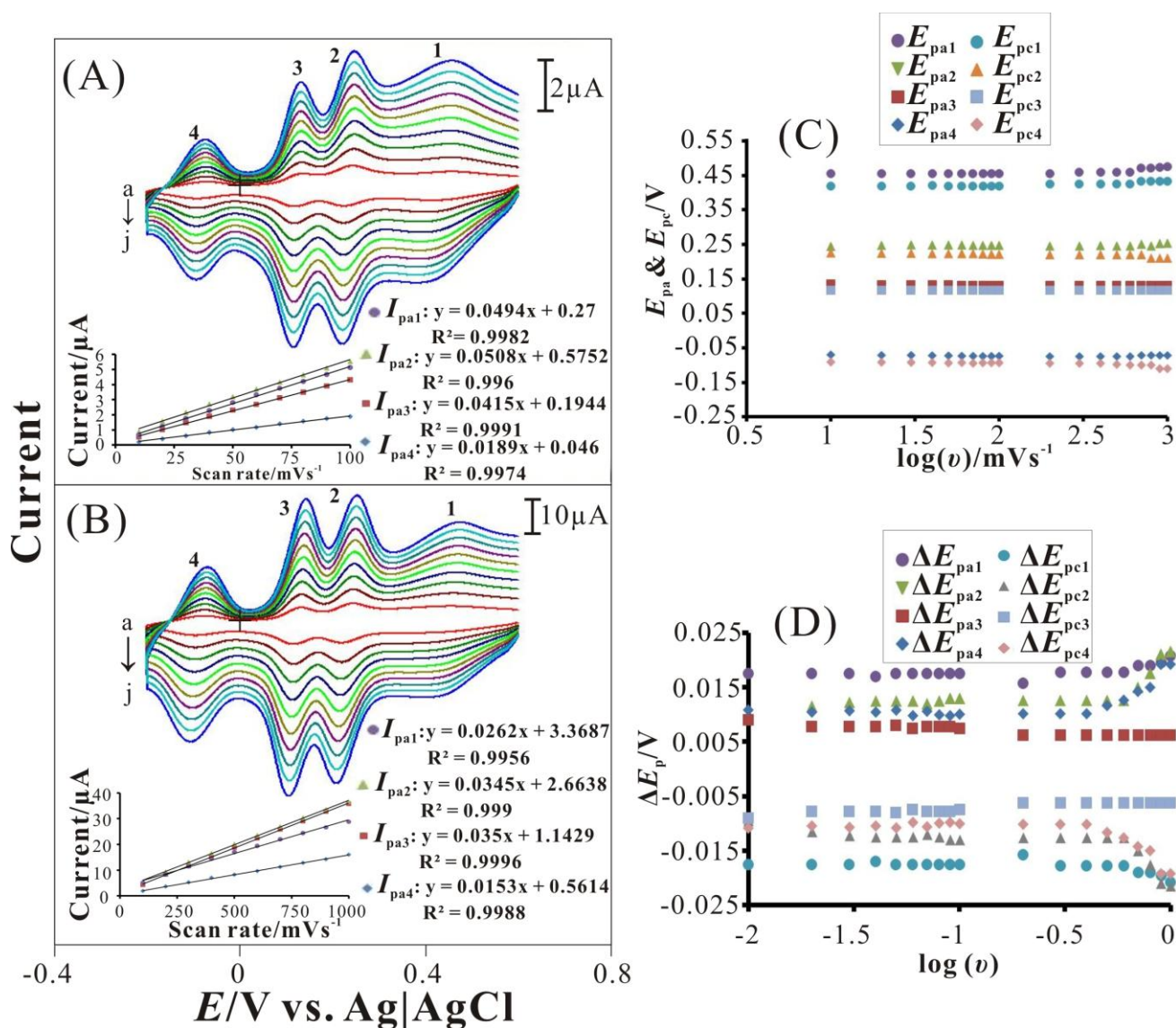

Figure 2. Cyclic voltammograms of PANI/SiMO/GCE examined in 0.1 M H$_2$SO$_4$ solution (pH 1.5) with (A) low scan rate of: (a) 10 , (b) 20, (c) 30, (d) 40, (e) 50, (f) 60, (g) 70, (h) 80, (i) 90, (j) 100 mV s^{-1}; and (B) high scan rate of: (a) 100 , (b) 200, (c) 300, (d) 400, (e) 500, (f) 600, (g) 700, (h) 800, (i) 900, (j) 1000 mV s^{-1}, respectively. Plots of (C) peak potential (E_{pa} & E_{pc}) and (D) peak potential change (ΔE_p) versus logarithmic scan rate (log(v)).

The influence of PANI/SiMO redox peaks on the scan rates was investigated. In the range of 10-100 mV s^{-1} (Fig. 2 A), both of the anodic and cathodic peak currents were proportional to the scan rate (peak 1 is used to study), implying that the electrochemical kinetics is a surface-controlled process. By comparison with low and high scan rate (insets of Fig. 2 A & B), the PANI/SiMO redox peak currents (I_p) were greatly enhanced with the increase of scan rate. Based on Laviron's equation [35] as following:

$$I_p = n^2F^2vA\Gamma/4RT \qquad (2)$$

where A (= 0.0707 cm^2) is the area of the glassy carbon electrode, n (= 2) is the number of electrons per reactant molecule, F is the Faraday constant, v is the scan rate, R is the gas constant, and T is the temperature. We assume that all of the immobilized redox centers are electroactive on the voltammetry time scale and a flat surface. From the slope of the I_p-v curve for a surface process, the surface concentration (Γ) of PANI was estimated. Under 20 scan cycles, the average surface concentration (Γ) of PANI was estimated about 1.37×10^{-10} mol cm^{-2}.

The dependence of the anodic peak potential (E_{pa}) and cathodic peak potential (E_{pc}) of the PANI/SiMO/GCE on the logarithmic scan rate (log(v)) in pH 1.5 sulfuric aqueous solution is depicted in Fig. 2C & D. At lower scan rates, E_{pa} and E_{pc} remained almost unchanged with the increase of scan rate. However, E_{pa} positively and E_{pc} negatively shifted at higher scan rates. At higher scan rates, the electron transfer coefficient (α) and the apparent surface electron transfer rate constant (K_s) can be obtained from Laviron theory [36]. The peak-to-peak potential separation ($\Delta E_p = E_{pa} - E_{pc}$) is about 40 mV for PANI and 30 mV, 20 mV, and 25 mV for SiMO redox peaks obtained below 100 mV s^{-1}, suggesting facile charge transfer kinetics over this scan rate. Based on Laviron theory [34], the electron transfer rate constant (K_s) and charge transfer coefficient (α) can be determined by measuring the variation of peak potential with scan rate. The values of peak potentials were proportional to the logarithm of the scan rate for scan rates higher than 500 mV s^{-1} (Fig. 2D). The slope of ΔE_p versus log(v) was about 37.3 mV for PANI and was about 43 mV for SiMO peak. Using the equation $E_p = K - 2.303(RT/nF)\log v$ and the two electrons transferred for PANI a charge transfer coefficient 0.60 was obtained. Introducing these values in the equation [35] as following:

$$\log K_s = \alpha \log(1 - \alpha) + (1 - \alpha)\log \alpha - \log(RT/nFv) - \alpha(1 - \alpha)nFE/2.3RT \qquad (2)$$

An apparent surface electron transfer rate constant (K_s) 1.878 s^{-1} was estimated for reversible redox peaks in PANI/SiMO/GCE.

Fig. 3 displays the pH-dependent voltammograms of PANI/SiMO modified electrode. In order to ascertain this, the voltammetric responses of PANI/SiMO electrode were obtained in the solutions of different pH values varying from 1 to 13. The formal potential of these redox couples are pH-dependent with negative shifting as increasing pH value of the buffer solution. The inset in Fig. 3 shows the formal potential ($E_1^{0'}$, $E_2^{0'}$, $E_3^{0'}$, and $E_4^{0'}$) of PANI/SiMO plotted over a pH range of $1-13$. $E_1^{0'}$, $E_2^{0'}$, $E_3^{0'}$, and $E_4^{0'}$ represent the formal potential from the positive side to the negative side. The response of PANI redox couple ($E_1^{0'}$) shows a slope of -64.2 mV/pH, which is close to that given by

the Nernstian equation for equal number of electrons and protons transfer processes. The SiMO redox couples ($E_1^{0'}$, $E_2^{0'}$, $E_3^{0'}$) shows a slope of -62.7, -77.4, and -69.8 mV pH^{-1}, respectively. They are close to that expected from calculations using Nerstian equation. The phenomenon indicates that the number of electrons and protons is the same. In our case, two electrons and one proton were involved in the PANI redox couple, whereas two electrons and two protons were involved in each SiMO redox couple. The above result shows that the PANI/SiMO hybrid film is stable and electrochemically active in the aqueous buffer solutions.
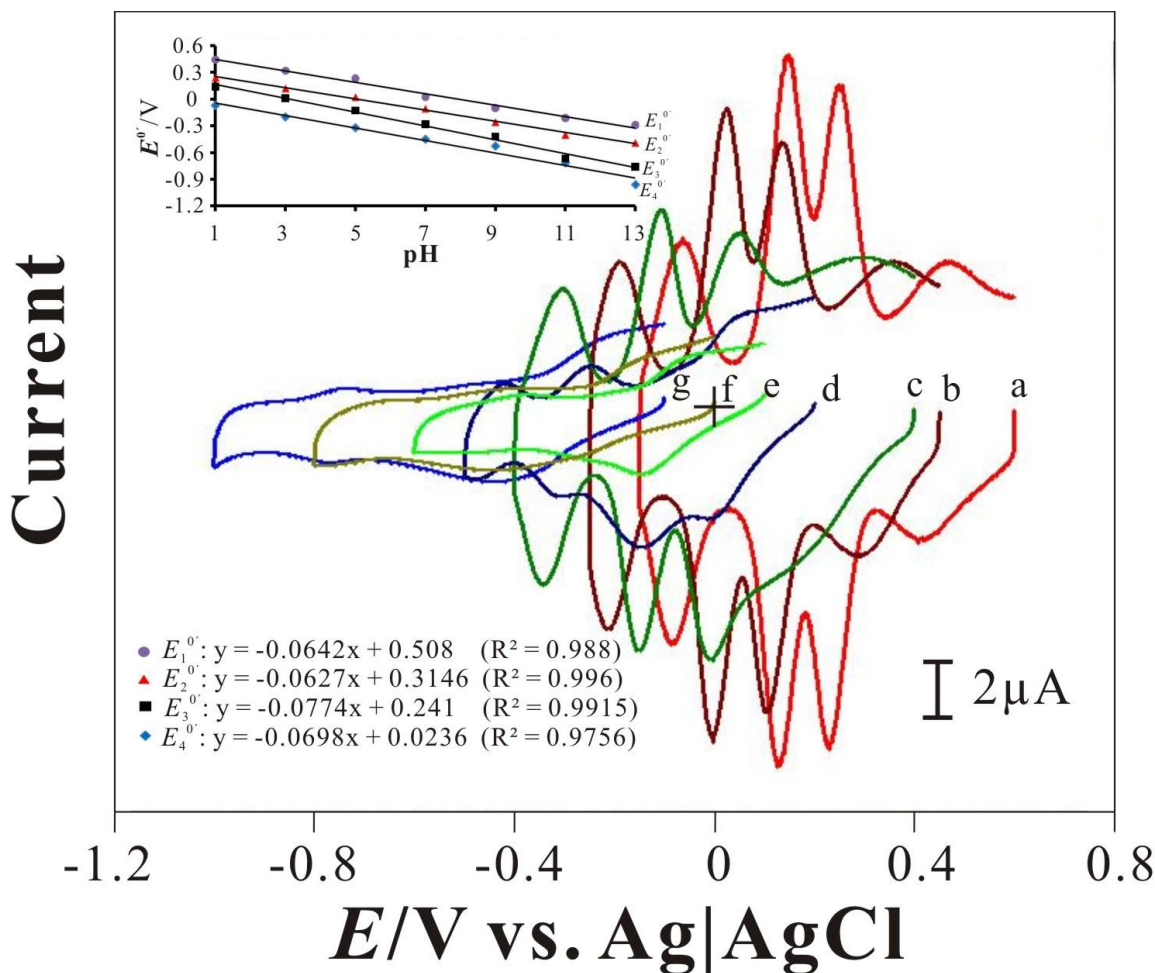

Figure 3. Cyclic voltammograms of PANI/SiMO/GCE examined in 0.1 Vs^{-1} with various pH conditions of: (a) pH 1, (b) pH 3, (c) pH 5, (d) pH 7, (e) pH 9, (f) pH 11, and (g) pH 13, respectively. Inset was the plot of formal potential of PANI/SiMO/GCE versus pH ($E_1^{0'}$, $E_2^{0'}$, $E_3^{0'}$, and $E_4^{0'}$ were the formal potential respected four redox couples of the modified electrode in the order from positive to negative potential).

3.3. UV-Vis spectra analysis

The experiment was designed to understand the spectra of these materials in the solution or coated on ITO by UV-Visible spectroscopy. Fig. 4B shows the spectra of these materials dissolved in 0.1 M H_2SO_4 buffer solution (pH 1.5).
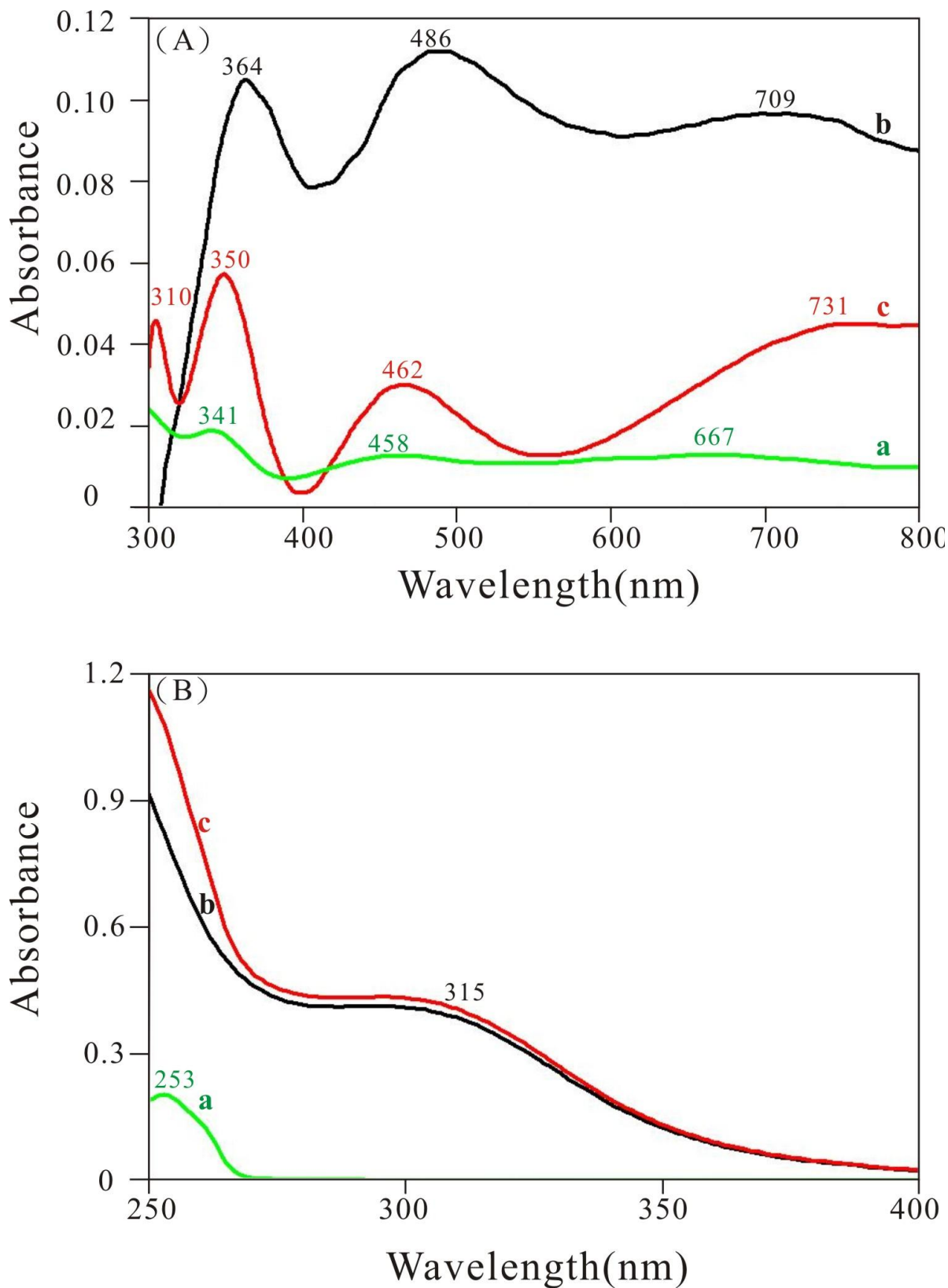
Figure 4. (A) UV-Vis spectra of (a) PANI/ITO, (b) SiMO/ITO, and (c) PANI/SiMO/ITO. (B) UV-Vis spectra of (a) 1×10^{-3} M aniline, (b) 2×10^{-5} M SiMO, and (c) 1×10^{-3} M aniline + 2×10^{-5} M SiMO examined in 0.1 M H_2SO_4 aqueous solution (pH 1.5).

Fig. 5B(a) is the aniline spectrum with one main absorption peak at about 253 nm revealing the aniline monomer.
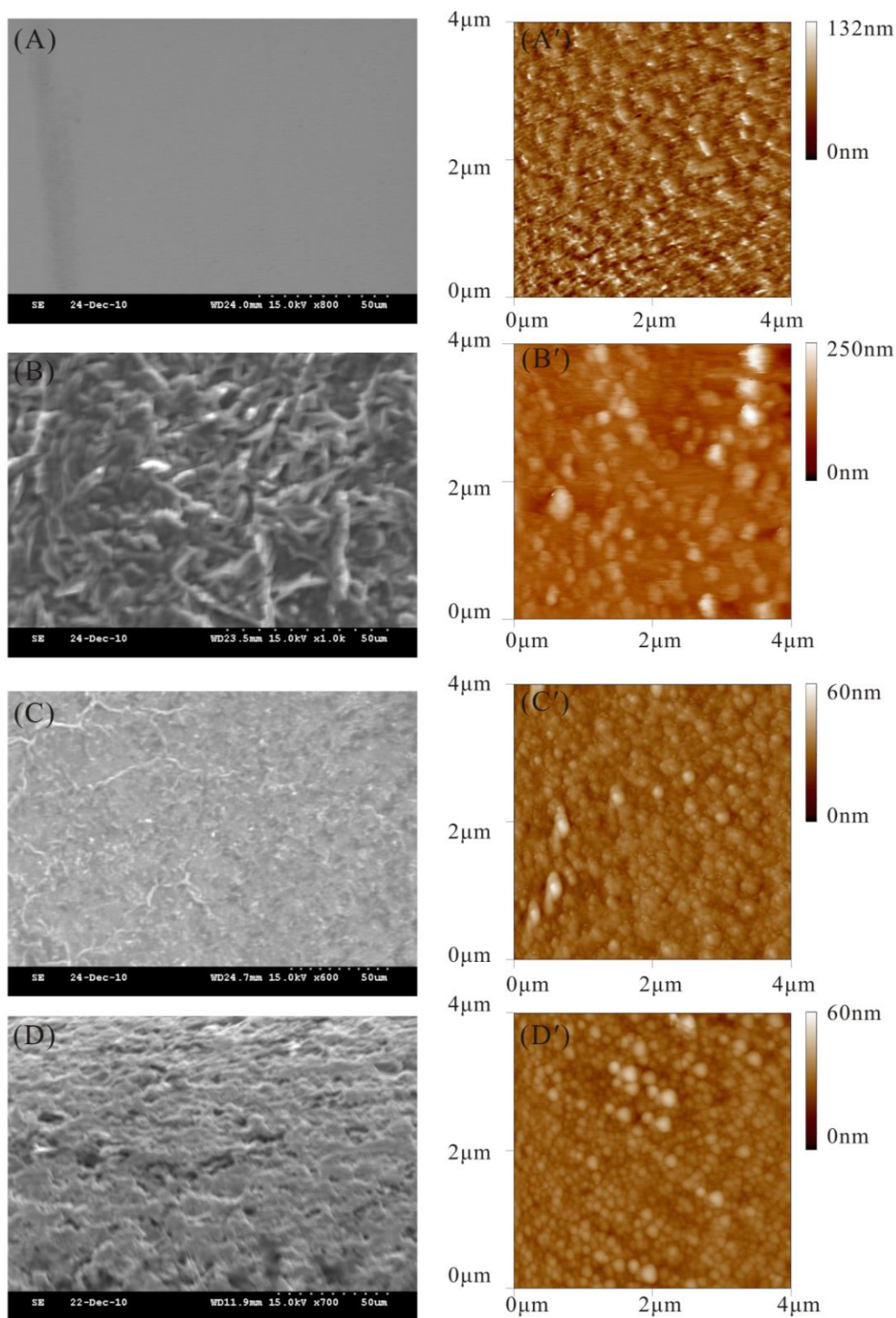

Figure 5. SEM image of (A) bare ITO, (B) SiMO/ITO, (C) PANI/ITO and (D) PANI/SiMO/ITO; tapping mode AFM image of (A') bare ITO, (B') SiMO/ITO, (C') PANI/ITO and (D') PANI/SiMO/ITO.

Fig. 5B(b) is the SiMO spectrum with the main absorption peak at 315 nm in the same condition. Furthermore, Fig. 5B(c) shows no new absorption peaks in the spectrum of aniline and SiMO mixture. It means that no interaction between aniline monomer and SiMO. Fig. 5A shows the UV-Vis spectra of (a) PANI/ITO, (b) SiMO/ITO, and (c) PANI/SiMO/ITO, respectively. It can be found that the absorption peaks are different from that of these materials in aqueous solution. PANI/ITO has main absorption peaks at 341 nm, 458 nm, and 667 nm. SiMO/ITO has main adsorption peaks at 364 nm, 486 nm, and 709 nm. As PANI/SiMO/ITO electro-codeposited by cyclic voltammetry, it has absorption peaks similar to the additional result of PANI/ITO and SiMO/ITO. It is noticed that the absorption peak height is lower than that of PANI/ITO. This might be due to the different deposition amount between PANI/SiMO (the electro-codeposition) and PANI (the electropolymerization). It can be concluded that there is no other chemical reaction between aniline and SiMO in the aqueous solution. PANI and SiMO can be co-deposited without other interaction in the electro-codeposition process. This PANI/SiMO film can be stably immobilized on electrode surface.

3.4. SEM and AFM characterization

Scanning electron microscopy (SEM) and atomic force microscopy (AFM) were utilized to study the morphology of the active surface of the electrodeposited PANI films with/without SiMO, and compared with the bare ITO substrate, as shown in Fig. 5. The bare ITO appears flat surface, in contrast with the SiMO, PANI, and PANI/SiMO film modified GCE electrodes, which has a relatively smooth surface in SEM images (Fig. 4A–D). The SiMO/ITO (SiMO coated on ITO by adsorption) exhibits specific crystalline shape might be due to the aggregation of SiMO molecules. The PANI/ITO (PANI coated on ITO by electropolymerization) has specific fiber-like structure might be due to the formation of PANI polymer chains. Particularly, the PANI/SiMO (co-immobilized by electropolymerization) shows unique porous surface different from SiMO and PANI. This is extremely like that some SiMO molecules cover over the PANI polymer chains. Compared with the corresponding AFM images (Fig. 5A'–D') of these films, they were estimated with average diameter of 26.2 nm, 29.7 nm, and 29.3 nm, and with average height of 57.6 nm, 71.6 nm, and 21.4 nm for SiMO, PANI, and PANI/SiMO, respectively. Except of average height, it can be noticed that PANI/SiMO particle size is the same as PANI. The hybrid composite might be dispersion through this process. This also might provide that the SiMO molecules cover over the PANI polymerized layer. One can conclude that the film formation of static interaction between PANI and SiMO leads to form a much compact structure.

3.5. Electrocatalytic properties of PANI/SiMO film modified electrode

The electrocatalytic oxidation of AA, DA, EP, and NEP using the PANI/SiMO hybrid film was investigated. Fig. 6 displays the cyclic voltammograms of these species electrocatalytic oxidation in various pH solutions (pH 0.55-4) by PANI/SiMO/GCE. The added amount was recorded in Table 1.

Comparing to bare GCE electrode (a'), which shows almost no electrocatalytic current response for these species in the same condition, this film modified electrode can show uniquely electrocatalytic potential and current.

Table 1. Species added data of PANI/SiMO/GCE electrocatalytic reaction in various pH conditions (raw data from Fig. 6 & 8).

Condition	pH 0.55 (0.5 M H_2SO_4)				pH 1.5 (0.1 M H_2SO_4)			pH 4 (0.1 M KHP)		
Species Added/mM	a	b	c	d	b	c	d	b	c	d
AA	0	1	2	3	0.5	1	1.5	1	2	3
DA	0	1	2	3	0.5	1	1.5	1	2	3
EP	0	1	2	3	1	2	3	2	4	6
NEP	0	1	2	3	1	2	3	1.5	3	4.5
$KBrO_3$	0	1	2	3	0.5	1	1.5	-	-	-
KIO_3	0	0.3	0.6	0.9	0.2	0.4	0.6	-	-	-
$NaNO_2$	0	2	4	6	2	4	6	-	-	-
$K_2S_2O_8$	0	1	2	3	1	2	3	-	-	-

Table 2. The electrocatalytic peaks of PANI/SiMO/GCE with various reactants in pH 0.55-4 aqueous solutions.

Condition	pH 0.55 (0.5 M H_2SO_4)	pH 1.5 (0.1 M H_2SO_4)	pH 4 (0.1 M KHP)
Substrate	Electrocatalytic peak potential, E_{pcat}[a]/ V		
AA	0.6	0.45	0.32
DA	0.6	0.45	0.32
EP	0.6	0.45	0.32
NEP	0.6	0.45	0.32
$KBrO_3$	-0.05	-0.12	-
KIO_3	-0.05, 0.17, 0.27	-0.12, 0.10, 0.22	-
$NaNO_2$	-0.05, 0.17, 0.27	-0.12, 0.10, 0.22	-
$K_2S_2O_8$	-0.05, 0.18, 0.25	-0.12, 0.10, 0.22	-

[a]E_{pcat}, the anodic or cathodic peak potential of the electrocatalytic reactions.

As shown in Table 2, PANI/SiMO/GCE has specific electrocatalytic peaks for these species in each case. These peaks are also noticed that the electrocatalytic peak current is dependent on pH condition of the solutions. Fig. 7 shows the plots of electrocatalytic peak current versus species concentration at different pH conditions. It can be found that this film has better electrocatalytic result in lower pH condition. As the result, PANI/SiMO hybrid film can be a good choice as a biochemical sensor to detect AA, DA, EP, and NEP.
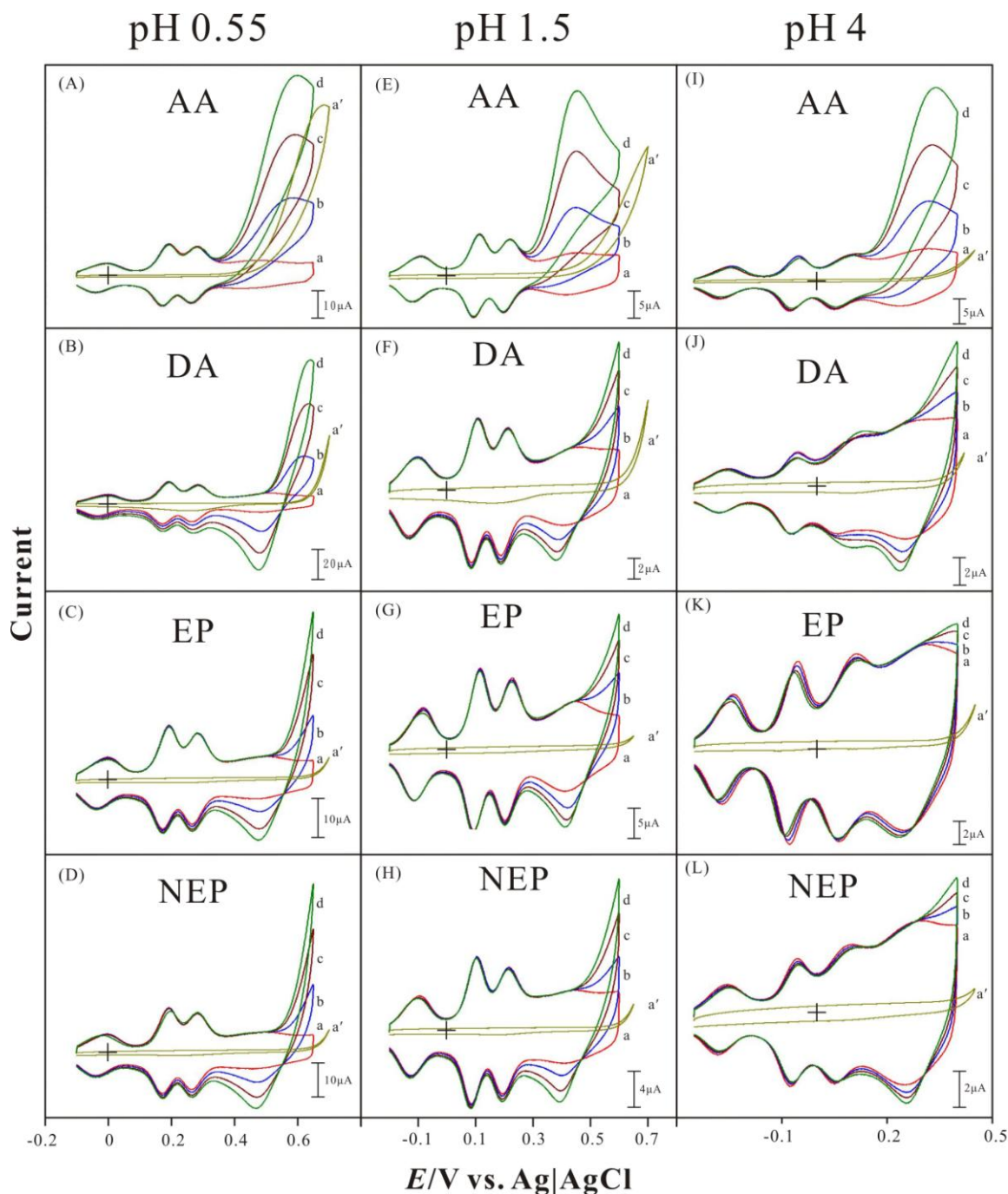
Figure 6. Cyclic voltammograms of PANI/SiMO/GCE examined in various pH solutions (pH 0.55, pH 1.5, pH 4) containing AA, DA, EP, and NEP, respectively. Scan rate = 0.1 V s^{-1}. Curve (b)-(d) were voltammetric response of PANI/SiMO/GCE with species additions, curve (a) was the background of the modified electrode and (a') was bare electrode examined in the presence of species with maximal added amount in each case. The added amount was recorded in Table 1.

The electrocatalytic reduction of bromate, iodate, nitrite, and persulfate using the PANI/SiMO hybrid film was investigated. Fig. 8 displays the cyclic voltammograms of these species electrocatalytic reduction at different pH conditions (pH 0.55-1.5) by PANI/SiMO/GCE. The added

amount was recorded in Table 1. It can be found that this electrode has specific electrocatalytic peaks in each case.
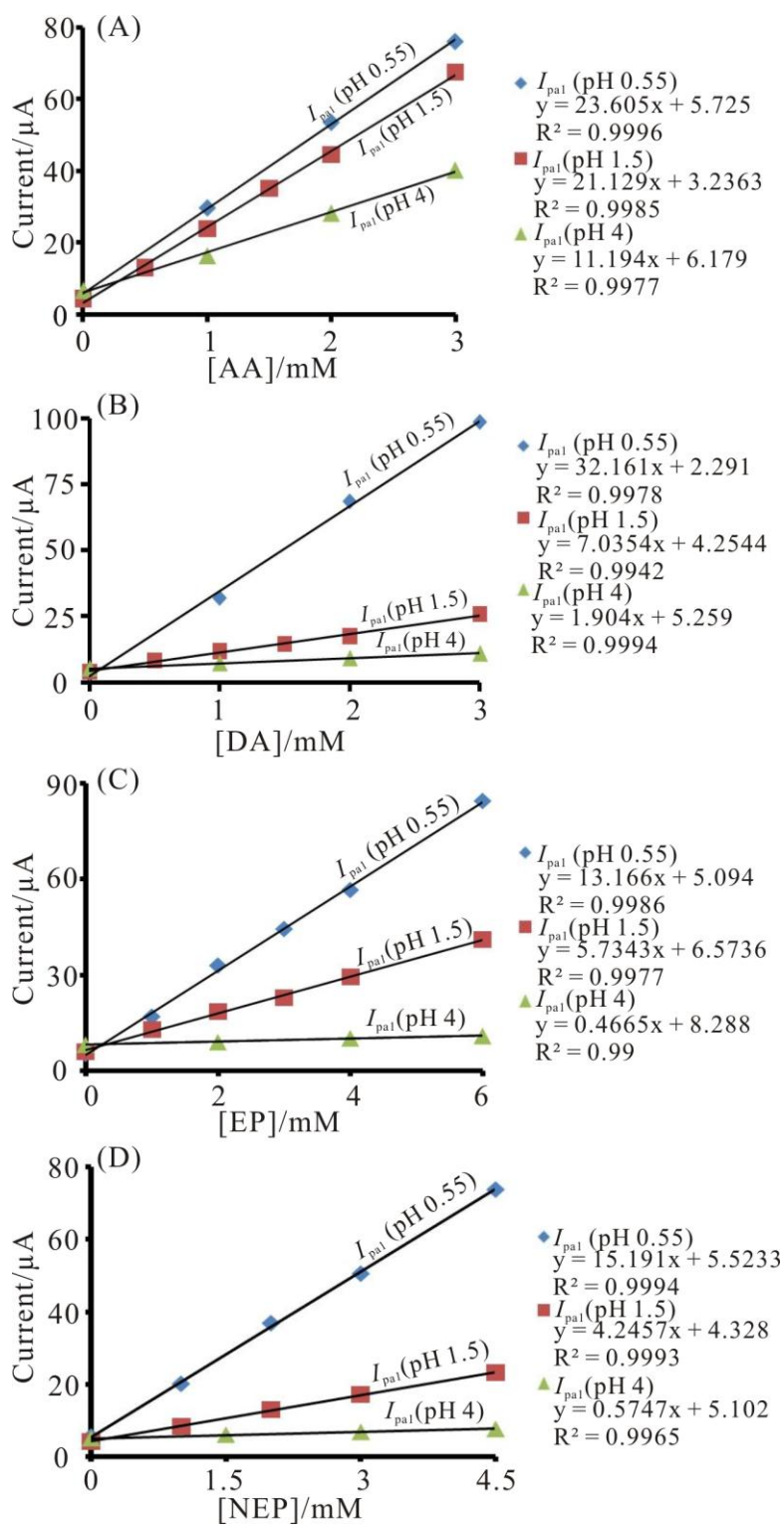

Figure 7. Plots of PANI/SiMO/GCE electrocatalytic peak current versus species concentration. PANI/SiMO/GCE examined in different pH conditions (pH 0.55, pH 1.5, and pH 4) in the presence of (A) AA, (B) DA, (C) EP, and (D) NEP, respectively.

The electrocatalytic peak current is dependent on species concentration with good linearity. As shown in Fig. 9, this electrode can show higher current response in pH 0.55 for these species except of persulfate. It exhibits electrocatalytic properties on the redox peaks. From above results, PANI/SiMO hybrid film is an electroactive material with both elctrocatalytic oxidation and reduction property particularly in lower pH condition.
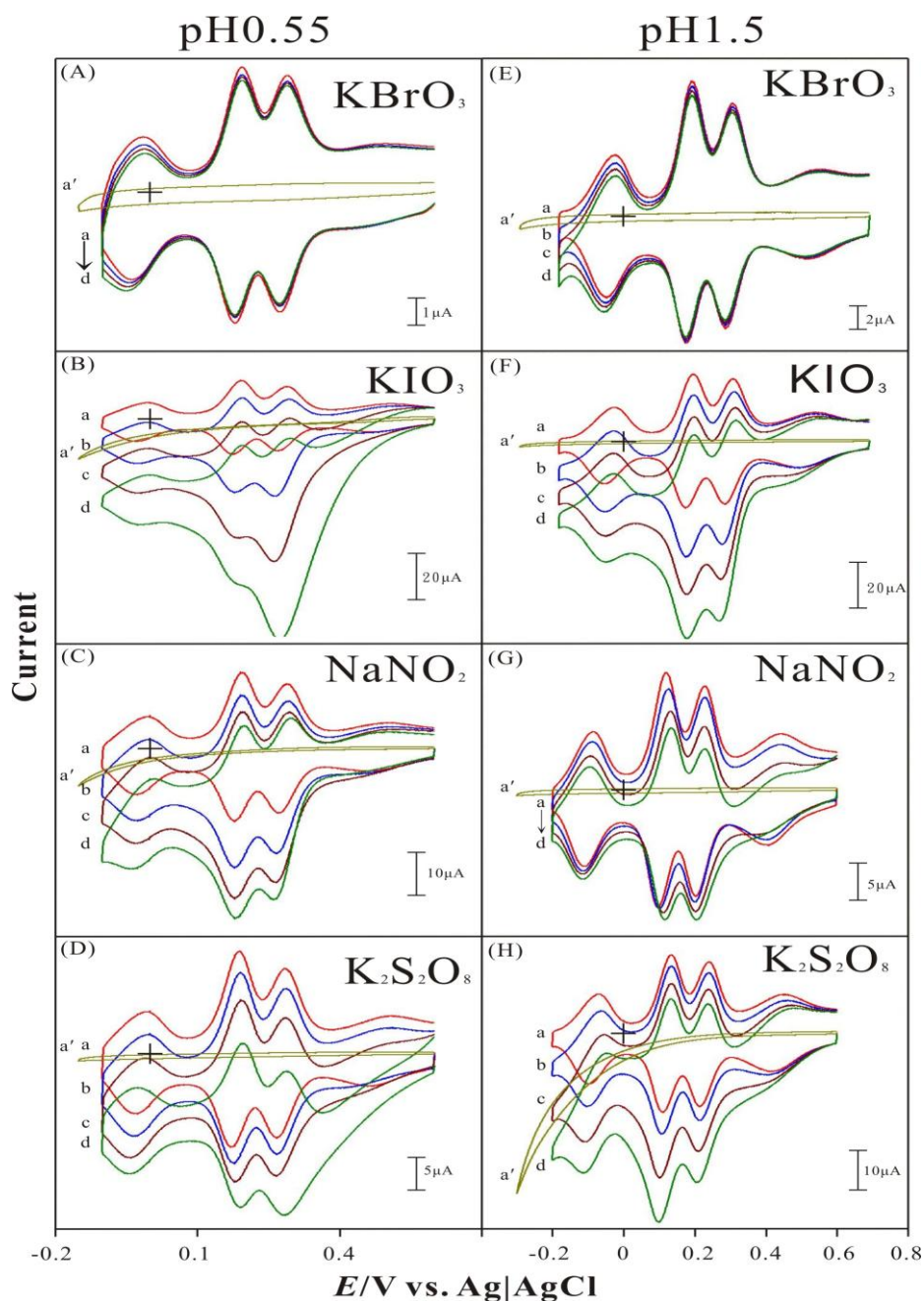

Figure 8. Cyclic voltammograms of PANI/SiMO/GCE examined in various pH solutions (pH 0.55, 1.5) containing (A) $KBrO_3$, (B) KIO_3, (C) $NaNO_2$, and (D) $K_2S_2O_8$, respectively. Scan rate = 0.1 V s^{-1}. Curve (b)-(d) were voltammetric response of PANI/SiMO/GCE with species additions, curve (a) was the background of the modified electrode and (a') was bare electrode examined in the presence of species with maximal added amount in each case. The added amount was recorded in Table 1.
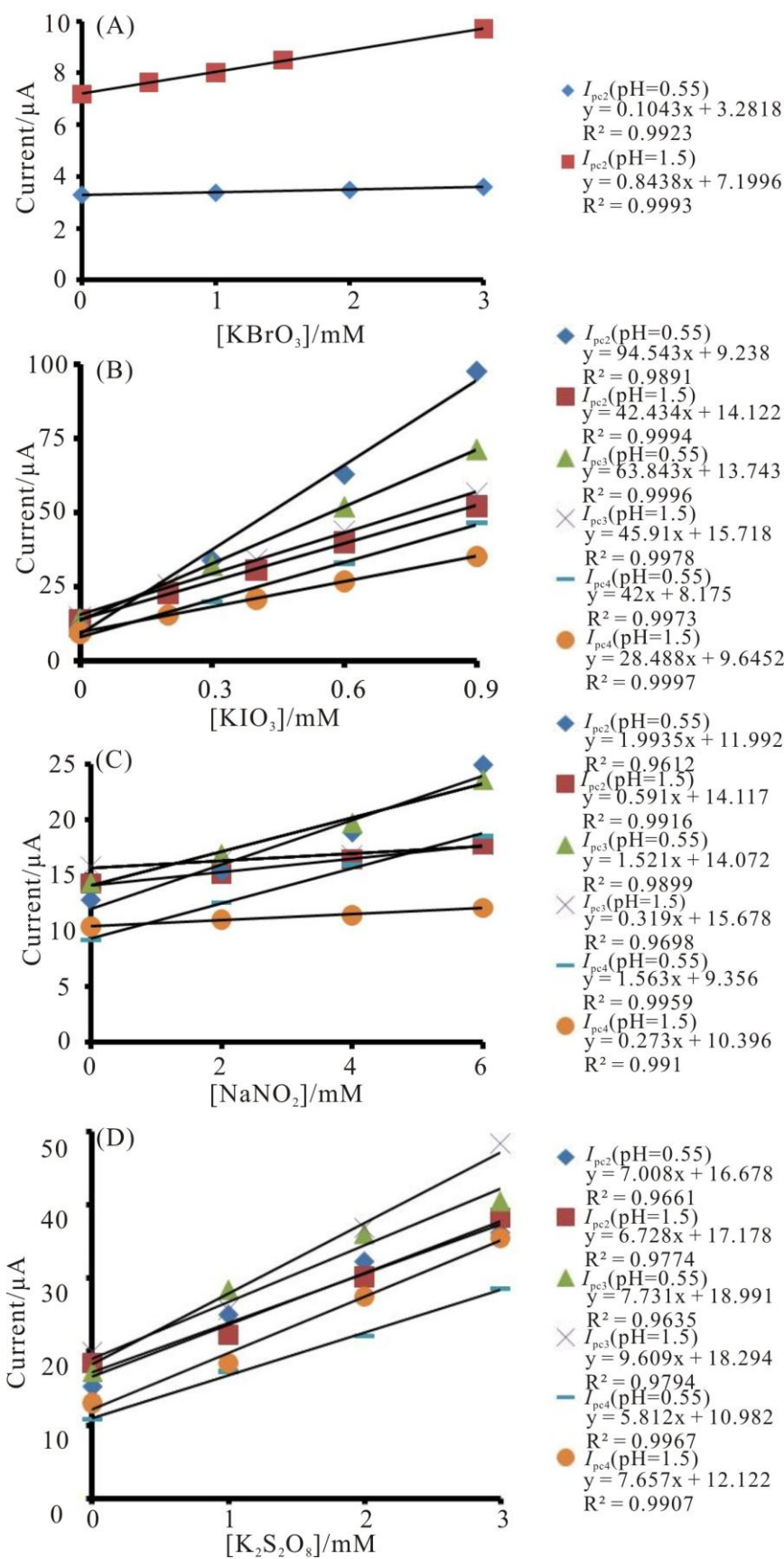
Figure 9. Plots of PANI/SiMO/GCE electrocatalytic peak current versus species concentration. PANI/SiMO/GCE examined in different pH conditions (pH 0.55, pH 1.5) in the presence of (A) KBrO$_3$, (B) KIO$_3$, (C) NaNO$_2$, and (D) K$_2$S$_2$O$_8$, respectively.
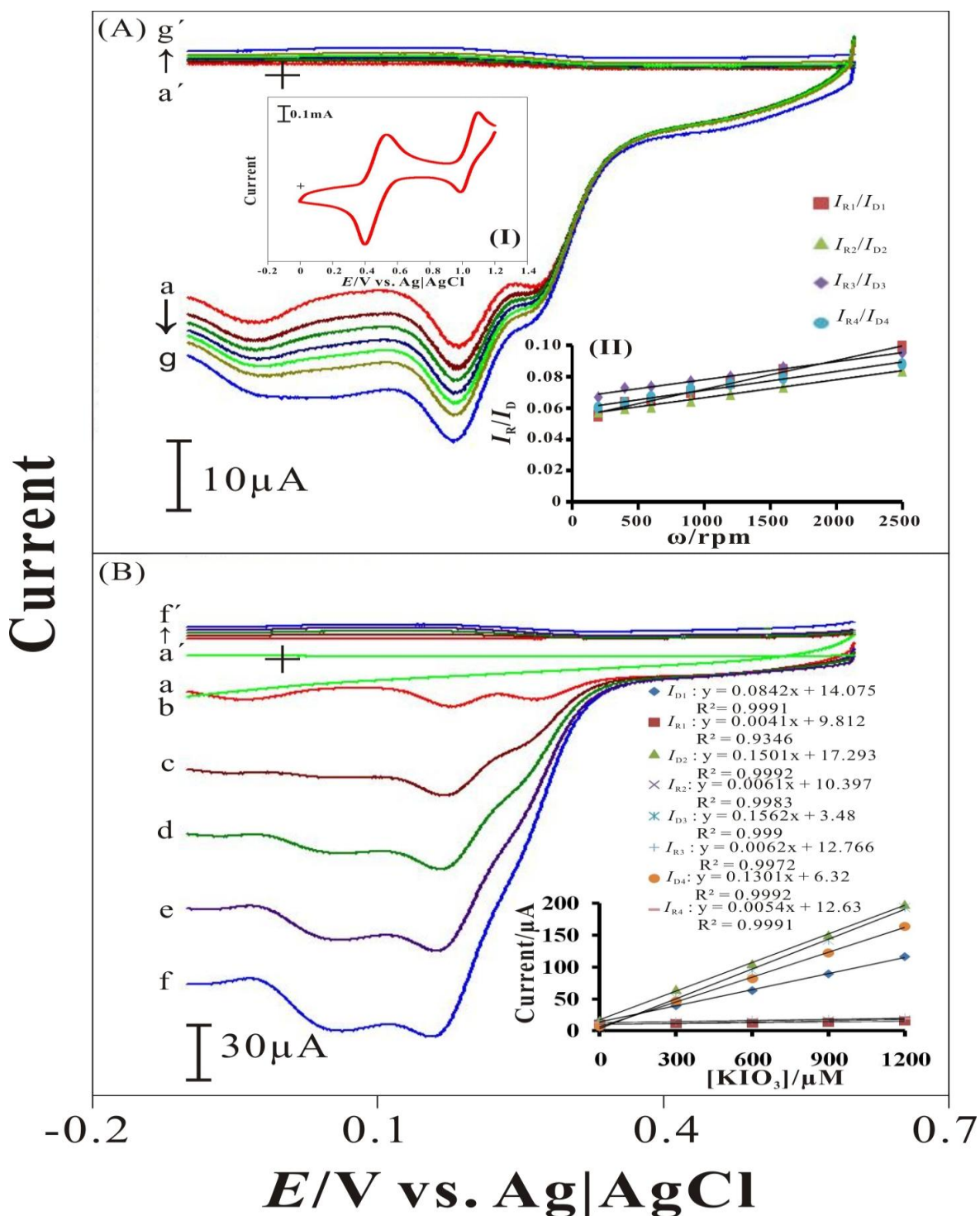
Figure 10. (A) RRDE voltammograms of PANI/SiMO hybrid film adsorbed on a glassy carbon disk electrode in 0.5 M H_2SO_4 solution (pH 0.55) containing 5×10^{-4} M IO_3^- with various rotation rates of: (a) 200 rpm, (b) 400 rpm, (c) 600 rpm, (d) 900 rpm, (e) 1200 rpm, (f) 1600 rpm, and (g) 2500 rpm, respectively. (B) RRDE voltammograms of PANI/SiMO hybrid film examined at rotation rate of 2500 rpm with various iodate concentrations of: $[IO_3^-] =$ (a) 0, (b) 3×10^{-4} M, (c) 6×10^{-4} M, (d) 9×10^{-4} M, (e) 1.2×10^{-3} M, respectively. Scan rate = 0.02 V s^{-1}. Platinum ring electrode (E_R = +1.1 V). Insets of (A) were (I) the cyclic voltammogram of 1×10^{-2} M iodide (pH 1.5) using bare glassy carbon electrode and (II) the plot of I_R/I_D versus $\omega^{1/2}$. Inset of (B) was the plot of I_D, I_R versus iodate concentration.

As result shown in Table 2, we conclude that the PANI/SiMO hybrid film is a good electroactive material due to good electrocatalytic reaction for AA, DA, EP, NEP, BrO_3^-, IO_3^-, NO_2^-, and $S_2O_8^{2-}$. It has potential to develop one novel multi-functional sensor for these species.

3.6. The electrocatalytic reduction of IO_3^- by a hybrid PANI/SiMO film using Rotating Ring-Disk Electrode

Fig. 10 shows the rotating ring-disk electrode measurements of the electrocatalytic reduction in the presence of IO_3^- using a hybrid PANI/SiMO film.

Fig. 10A shows the rotating ring-disk electrode measurements of 5×10^{-4} M IO_3^- reduction was carried out using a PANI/SiMO modified disk electrode with rotation rate of 2500 rpm. We predict that iodide is the product of iodate reduction in this case, a ring electrode potential was set at $E_R = 1.1$ V based on the cyclic voltammogram of 1×10^{-2} M I^- (inset of Fig. 10A). The product analysis of the iodate electrocatalytic reduction was performed by PANI/SiMO film modified disk electrode. The collection efficiency, $N = I_R/I_D$, was obtained about 0.08 for the iodate electrocatalytic reduction by PANI/SiMO film.

Fig. 10B shows the rotating ring-disk electrode measurements conducted for five iodate concentrations. The iodate reduction was carried out with a rotation rate of 2500 rpm and $E_R = 1.1$ V. The inset plot (II) shows both I_D and I_R as a function of the concentration of IO_3^- in the solution. The results show that the IO_3^- was reduced to I^-. The product analysis results were also consistent with the results using the rotating ring-disk electrode method.

3.7. Stability study of PANI/SiMO film modified electrode

Repetitive redox cycling experiments were done to determine the extent of stability relevant to PANI/SiMO modified GCE in 0.1 M H_2SO_4 solution (pH 1.5). This investigation indicated that after 100 continuous scan cycles with scan rate of 0.1 Vs^{-1}, the peak heights of the cyclic voltammograms decreased less than 5%. On the other hand, the PANI/SiMO modified GCE kept its initiate activity for more than one month as kept in 0.1 M H_2SO_4 solution (pH 1.5). A decrease of 4% was observed in current response of the electrode at the end of 30th day.

4. CONCLUSIONS

Here we report a simple method to electrochemically co-deposit poly(aniline) and SiMO nanocomposites. This hybrid film modified electrode is characterized in stable with various scan rates in acidic aqueous solutions. No chemical reaction occurs between poly(aniline) and SiMO after electro-codeposition. The film surface is getting flat different from SiMO. This modified electrode maintains both electrocatalytic oxidation and reduction properties to various species including important biological molecules and oxide species. It also shows much better electrocatalysis in strong

acidic aqueous solutions. This electrode is good to develop a multifunctional sensor for the determination of AA, DA, EP, NEP, NADH, BrO_3^-, IO_3^-, NO_2^-, and $S_2O_8^{2-}$.

References

1. Y.S. Negi, P.V. Adhyapak, *Polym. Rev.* 42 (2002) 35-53
2. S. Bhadra, D. Khastgir, N.K. Singha, J. HeeLee, *Prog. Polym. Sci.* 34 (2009) 783-810
3. N. Oyama, T. Tatsuma, T. Sato, T. Sotomura, *Nature* 373 (1995) 598-600
4. S. Mu, J. Ye, Y. Wang, *J. Power Sources* 45 (1993) 153-159
5. P.K. Rajendra, N. Munichandraiah, *Anal. Chem.* 74 (2002) 5531-5537
6. M. Kanungo, A. Kumar, A.Q. Contractor, *Anal. Chem.* 75 (2003) 5673-5679
7. L. Zhang, X. Jiang, S. Dong, *Biosens. Bioelectron.* 21 (2006) 1107-1115
8. L. Zhang, J.Y. Lian, *J. Electroanal. Chem.* 611 (2007) 51-59
9. L. Zhang, *J Solid State Electrochem.* 11 (2007) 365-371
10. F. Xiao-juan, S. Yan-long, H. Zhong-ai, *Int. J. Electrochem. Sci.* 5 (2010) 489-500
11. C.C. Yang, T.Y. Wu, H.R. Chen, T.H. Hsieh, K.S Ho, C.W. Kuo, *Int. J. Electrochem. Sci.* 6 (2011) 1642-1654
12. J. Yue, A.J. Epstein, *J. Am. Chem. Soc.* 112 (1990) 2800-2801
13. I.Mav, M. Zigon, A. Sebenik, Vohlidal, *J. Polym. Sci. Part A: Polym. Chem.* 38 (2000) 3390-3398
14. S. Mu, J. Kan, *Synth. Met.* 132 (2002) 29-33
15. L.V. Lukachova, E.A. Shkerin, E.A. Puganova, E.E. Karyakina, S.G. Kiseleva, A.V. Orlov, G.P. Karpacheva, A.A. Karyakin, *J. Electroanal. Chem.* 544 (2003) 59-63
16. L. Zhang, S. Dong, *J. Electroanal. Chem.* 568 (2004) 189-194
17. X. Wang, Z. Kang, E. Wang, C. Hu, *J. Electroanal. Chem.* 523 (2002) 142-149
18. L. Cheng, J.A. Cox, *Electrochem. Commun.* 3 (2001) 285-289
19. L.M. Abrantes, C.M. Cordas, E. Vieil, *Electrochim. Acta* 47 (2002) 1481-1487
20. S. Dong, L. Cheng, X. Zhang, *Electrochim. Acta* 43 (1998) 563-568
21. M. Barth, M. Lapkowski, S. Lefrant, *Electrochim. Acta* 44 (1999) 2117-2123
22. D. Martel, A. Kuhn, P.J. Kulesza, M.T. Galkowski, M.A. Malik, *Electrochim. Acta* 46 (2001) 4197-4204
23. L. Cheng, S. Dong, *J. Electroanal. Chem.* 481 (2000) 168-176
24. P.J. Kulesza, M. Chojak, K. Miecznikowski, A. Lewera, M.A. Malik, A. Kuhn, *Electrochem. Commun.* 4 (2002) 510-515
25. T.R. Zhang, W. Feng, R. Lu, X.T. Zhang, M. Jin, T.J. Li, Y.Y. Zhao, J.N. Yao, *Thin Solid Films* 402 (2002) 237-241
26. J. Bergquist, A. Sciubisz, A. Kaczor, J. Silberring, *J. Neurosci. Methods* 113 (2002) 1–13
27. E.L. Bravo, R.W. Gifford, *N. Engl. J. Med.* 311 (1984) 1298–1303
28. H. Wisser, E. Knoll, *Internist.* 28 (1987) 123–127
29. D.J. Boullin, C.B.T. Adams, J. Mohan, *Neuropathol. Appl. Neurobiol.* 2 (1976) 491–1491
30. M. Frankenhaeuser, *Brain Res.* 31 (1971) 241–262
31. I.A. Macdonald, D.M. Lake, *J. Neurosci. Methods* 13 (1985) 239–248
32. C. Sabbioni, M.A. Saracino, R. Mandrioli, S. Pinzauti, S. Furlanetto, G. Gerra, M.A. Raggi, *J. Chromatogr. A* 1032 (2004) 65–71
33. L.A. Pachla, D.L. Reynolds, P.T. Kissinger, *J. Assoc. Off. Anal. Chem.* 68 (1985) 1–12
34. Y.T. Chang, K.C. Lin, S.M. Chen, *Electrochim. Acta* 51 (2005) 450–461

35. E. Laviron, *J. Electroanal. Chem.* 52 (1974) 355-393
36. E. Laviron, *J. Electroanal. Chem.* 101 (1979) 19-28